Evolution of Microstructure and Crystalline Texture in Aluminum Sheet Metal Subjected to High Strain Rate Biaxial Deformation

by

Isaac Benjamin Feitler

Submitted to the Department of Materials Science and Engineering
in partial fulfillment of the requirements for the degree of

Bachelor of Science in Materials Science and Engineering

at the

MASSACHUSETTS INSTITUTE OF TECHNOLOGY

January 2005
[June 2005]

Author .....
Department of Materials Science and Engineering
January 14, 2005

Certified by .....
Christopher Schuh
Assistant Professor
Thesis Supervisor

Accepted by .....
Professor Caroline A. Ross
Chairman, Department Committee on Undergraduate Students

Evolution of Microstructure and Crystalline Texture in Aluminum Sheet Metal Subjected to High Strain Rate Biaxial Deformation

by

Isaac Benjamin Feitler

Submitted to the Department of Materials Science and Engineering
on January 14, 2005, in partial fulfillment of the
requirements for the degree of
Bachelor of Science in Materials Science and Engineering

Abstract

Electrohydraulic forming was used to biaxially stretch commercial Aluminum 5052 sheet metal workpieces at a high strain rate. Annealed and unannealed workpeices were formed. Specimens were taken from unformed metal and from the formed workpieces. Microstructures were examined with optical microscopy and pole figures were generated from X-ray diffraction data. Microstructures and crystalline textures were compared between formed and unformed and annealed and unannealed metal specimens, and strains were measured from the formed workpieces.

Thesis Supervisor: Christopher Schuh
Title: Assistant Professor

Acknowledgments

The author would like to acknowledge the following people for their role in his education and their help with the completion of this thesis:

Chris Schuh, Bernhardt Wuensch, Dwayne Daughtry, Joseph Dhosi, Ayida Mthembu, David Bono, Joe Parse, Meri Treska, Yin-Lin Xie, Toby Bashaw, Fred Cote, Joe Adario, Alan Lund, Megan Frary, Yet-Ming Chiang, Hao Hu, Rachel Sharp, Corinne Packard, Chris Ng, David Schoen, Jeremy Mason, Shelly Davis, John Cox, Richard Shyduroff, Peter Morley & the MIT Central Machine Shop, The Timken Company, Z Corp, Herb & Shirley Feitler, Bill & Sarah Hull, David & Zanna Feitler, Jacob Feitler

Contents

List of Figures

List of Tables

Chapter 1

Introduction

Materials processing and manufacturing techniques often introduce anisotropy to materials, or modify existing states of anisotropy. Anisotropy is the state of having the properties of a material depend on directionality of the material. A simple example of an anisotropic material is wood, which can be very strong under some kinds of stress, but which also splits easily along its grain. Without an understanding of the anisotropic properties of wood, woodworking would be next to impossible. Anisotropy in other materials, like metals, may not be as noticeable or easy to visualize with everyday examples, but it is still important.

Predicting the effects of processing techniques and the resulting properties of processed metals requires an understanding of the changes in the state of anisotropy. In turn, there must be ways to study and measure the degree and character of the anisotropy in metals, and ways to explain the transition from one state of anisotropy to another. One of the many ways to examine anisotropy in metals is the common metallographic technique of examining the shape of the microscopic crystal grains that make up the metal, also known as the microstructure. Another way is to use diffraction techniques to examine the distribution of the orientation of the grains, also known as the texture.

In a metal that is isotropic, where the properties are the same in all directions, the grains of the metal are as long as they are wide as they are deep, and the orientations of the grains are random with respect to each other. In an anisotropic

metal, the grains might be elongated or squashed, in which case the metal is said to morphologically anisotropic. A metal would be said to be crystallographically anisotropic if more grains were oriented towards some directions and less towards others. The terms 'crystalline texture' and 'preferred orientation' are also used to describe crystallographic anisotropy. It is common to see both morphological and crystalline anisotropy simultaneously in a metal. Changing the shape of a piece of metal macroscopically changes the shape of the grains in that piece of metal, and also changes the orientation of those grains. When a crystal grain of metal is deformed, planes of atoms in the crystal grains of the metal must slip past one another, and certain crystal planes, oriented in certain directions, slip more easily than others. To accommodate deformation, the orientation of a crystal grain may rotate so that the planes that slip most easily become more in line with the direction of the deformation.[1]

The changes in microstructure and crystalline texture due to various types of deformation have been studied, but the author is unaware of experimental study combining biaxial deformation at a high strain rate with empirical measurements of crystalline texture.[2, 3, 4] Biaxial deformation means stretching something in two directions at once; an example of biaxial stretching that is easy to visualize is the stretching of the skin of a balloon as it is inflated. High strain rate deformation simply means that the deformation happens very quickly. It is interesting because in some metals, deformation at a high strain rate allows the metal to be stretched farther before it breaks than it could if it were being stretched slowly.[5] One good way to produce high strain rate biaxial deformation in sheet metal is with an explosion, since the rapid pressure wave of an explosion can force a metal to stretch like the skin of a balloon very quickly. This the basis of this work: an explosion is used to deform aluminum workpieces at a high strain rate, and then the microstructure and crystalline texture of samples taken from the workpieces are examined.

The inspiration for this work comes from a class project to simply conduct high strain rate metal forming. There are many methods for high strain rate forming, but the one chosen was electrohydraulic forming, where a powerful electrical discharge

through a water-filled pressure vessel generates an explosive pressure wave that deforms a workpiece. The class project was successful, but did not study the results of the forming in much detail. Some additional details about this class project are presented in Appendix A.

Chapter 2

Experimental Methods

2.1 Materials

Sheets of 0.040 inch thick 5052 Aluminum metal with a 'mirror' finish were purchased from McMaster-Carr industrial supply. The mirror finish was chosen with the hope that it would be easy to apply a grid with precise spacing to the smoother surface, and that, and that the smoother finish might also make metallographic preparation of the metal easier. The aluminum was cut on a sheet metal brake into 8-inch square workpieces. Some workpieces were left unannealed (as recieved) and others were annealed in air. For the annealed workpieces, the annealing history was as follows: 345 C for 2 hours, 345 C for 3 hours, and then 450 C for 2 hours. In each annealing, the workpieces were raised to and lowered from the annealing temperature at a rate of 10 C per minute. This pattern of annealing was chosen so that the annealed mirror-finish workpieces ultimately felt the same when compared to annealed workpieces from the prior project in electrohydraulic forming. For that project, 0.040 inch thick 5052 Aluminum with a 'satin' finish had been purchased from McMaster-Carr, and the workpieces of it were annealed based on the listing for 5052 Aluminum in the ASM Metals Handbook, which gave an annealing temperature of 345 C and indicated that holding at that temperature was not required to anneal the metal.[6] After annealing, the satin-finish workpieces were noticeably easy to bend at the corner between thumb and forefinger, while the unannealed satin-finish workpieces were too stiff to bend

by hand this way. With the mirror-finish samples for this work, the unannealed workpieces felt as stiff as the unannealed satin-finish workpieces, but after the first treatment at 345 C for 2 hours, the annealed mirror-finish workpieces did not feel anywhere near as soft as the annealed satin-finish workpieces. The annealed mirror-finish workpieces still did not feel like the annealed satin-finish workpieces after the second annealing treatment, but after the third annealing treatment, conducted at a higher temperature, the annealed mirror-finish workpieces felt similar to the annealed satin-finish workpieces.

2.2 Pre-forming preparation

One of the goals of the work was to measure the amount the sample is strained at any given point on it's surface, and the most straightforward way to do this is to apply a visible grid to the surface that will deform as the workpiece deforms. Several approaches were considered to accomplish this, including drawing the grids on with a permanent marker, applying a coating to the workpiece and then scratching that coating off to mark a grid. The approach that was used for this work went with an iron-on transfer method for applying the grid to the workpiece. A grid for the workpieces was designed with drawing software, and printed onto Xerox™ Color Inkjet Iron-On Transfers. A hot clothes iron was used to apply these transfers to several annealed and unannealed workpieces. This method transferred the grid image to the workpieces by covering the workpieces with a film of plastic bearing the grid image. The transfer was not perfectly precise, and the transferred film was cracked in some places and distorted without cracking in others. After the grids were applied, the workpieces were photocopied, to preserve a record of the flaws in the applied grids before the workpieces were formed, in case those flaws became relevant later.

2.3 Forming

The workpieces were formed using the equipment from the previous electrohydraulic forming project. The equipment consisted of a custom-made electrohydraulic pressure vessel and matching expansion tube for the workpiece, neoprene rubber gaskets and padding between touching surfaces, a laboratory press to hold the pressure vessel, expansion tube, gaskets, padding, and the workpiece together, an old Magneform machine serving as a capacitor bank, and a current monitor and voltage probe connected to oscilloscopes, connected in turn to a computer running National Instruments™ LabView™ data acquisition software. Forming was conducted with the Magneform set to full power. Electrical data from the current pulses was acquired using the LabView software. Additional details about the forming equipment and process are included in Appendix A.

2.4 Metallographic preparation

2.4.1 Sampling

For metallography, small specimens for of unformed metal were cut from unannealed and annealed metal sheets with tin snips. Specimens were cut from annealed and unannealed formed workpieces using an abrasive waterjet cutter, to avoid heating the metal, and to avoid causing any further deformation to the workpieces or the specimens cut from them. The workpieces were cut with the waterjet so that the specimens hung by a thin tab. The tab prevented the specimens from falling down into the sludge of the waterjet tank, and also provided a reference for the rolling direction of the workpiece after the specimen was broken off from the workpiece.

2.4.2 Mounting

Metallographic specimens were mounted in Buehler Probemet conductive molding compound, using a Buehler Simplimet 3 mounting press. The parameters for the

mounting process were 5 minutes duration, a temperature of 150 Celsius, and a pressure of 4200 PSI. Conductive molding compound was chosen because it would facilitate any attempts to perform Electron Back-Scattered Diffraction on the specimens in the mounts.

Mounts were prepared with two specimens in each mount. One specimen was laid flat, and the other specimen was held edge-on to the face of the mount with a stainless steel or plastic clip. For each mount, the orientations of the specimens were recorded before mounting, in terms of which surface of the sheet metal was on the face of the mount, and how the rolling direction of each specimen was oriented.

After mounting, the backs of the mounts were marked with a vibrating engraving pen, and the edges of the mount were beveled on a coarse grinding wheel.

2.4.3 Grinding and Polishing

The metallographic mounts were ground and polished with standard procedures. At typical grinding and polishing regimen would work down from 400 grit grinding papers through 600 grit and sometimes 800 and 1200 grit papers, before polishing was begun. Polishing usually began 1-micron diamond polishing media on Buehler brand MicroCloth cloths, then went to 0.3 micron alumina media on MicroCloth, and finished with a water-based colloidal silica media on TexMet cloth. Between grinding steps, the samples were rinsed with tap water and soap, and cleaned ultrasonically in soapy water for up to 5 minutes. Between polishing steps, it was found that rinsing with distilled water and cleaning ultrasonically in methanol helped keep the mounts clean and free of scratches. It took some and variation to find the proper procedure for polishing these particular mounts, and to develop the skill with these procedures to reliably produce a good polish on the mounts.

2.4.4 Etching

To reveal the grain structure of the metal, electrochemical etching was used. The final procedure was based on a Barker's etch, but modified by trial and error. Barker's

Etch consists of anodizing the mount at 20 V in Barker's Reagent, which is 4-5 mL of 48Acid (HBF4) in 200 mL of water.[7] For this work, 6mL of pure Fluoboric Acid in 194 mL of water was used, and the anodization was performed at a constant 31 V. A piece of 5052 Aluminum was cut from an unformed annealed sheet to be used as the cathode. For some etches, a graphite rod was used for the cathode instead. A typical etch time was 30 seconds. Polished mounts were prepared for etching by masking the face of the mounts with Kapton® tape, so that only the metal of the specimens remained exposed. Kapton® tape was also used to cover the other surfaces of the mount that might otherwise come into contact with the etchant solution while dipping the mount. An exposed copper wire was taped to the back of the mount, and a multimeter was used to check for electrical continuity between the wire and the exposed metal of the specimens on the face of the mount. After preparing the mount, all etching operations were performed inside a fume hood. To perform the etch, a bias of 31V was applied across the electrodes, with the mount as the anode and the piece of aluminum as the cathode, and the the mount was dipped face-down into the etchant solution for approximately seconds. A magnetic stirrer was used in the etchant bath to encourage uniform concentration of the etchant and to discourage the formation or deposition of bubbles on the mount being etched. After the etching dip, each mount was dipped sequentially into two beakers of distilled water to rinse off the etchant, and was washed more thoroughly outside the fume hood later. The tape was removed from each mount, and each mount was rinsed with methanol and dried off with air. The mounts were then examined with an optical microscope.

After the barkers etch, grain boundaries were faintly visible to the naked eye when tilting the mounts in normal lighting conditions, but no contrast was visible between grains. Examined with an optical microscope at various magnifications, no grains or grain boundaries were visible under brightfield illumination. With a polarizing filter in place on the microscope, contrast between grains became visible when another polarizing filter was rotated to 45 degrees. A digital camera attached to the microscope was used to capture photomicrographs of the specimens on the mounts. For some of the mounts, applying an orange filter improved the contrast

seen by the camera. Grain sizes were determined from photomicrographs of the mounted samples by the linear intercept method.

2.5 Strain Measurements

In-plane strains were measured from the grids of points that had been transferred to the workpieces. A dial caliper was used to measure the distance between points on the grids on the workpieces by placing the points of the jaws of the caliper on the two points being measured. Measurements were taken between points five grid points apart, because the spacing between individual points on the grid was to small to measure with accuracy or precision. Achieving accuracy and precision in the measurements was difficult even when measuring across five points at once. Strains in the thickness direction were measured simply by applying the caliper to representative portions of the workpieces. The annealed workpiece had been bisected when cutting the specimens for metallographic preparation, making it easy to measure the thickness at the area of interest. The unannealed workpiece was left substantially intact after the two specimens for metallography were cut out, and so direct measurement with the calipers was not convenient. Instead, a small strip of metal left behind when the metallographic specimens were removed was cut from the workpiece and measured directly with the caliper.

2.6 Electron Backscatter Diffraction

Electron Backscatter Diffraction (EBSD) on a polished mount was attempted in an FEI/Philips XL30 FEG ESEM, but the mount was not well enough polished to attain a usable diffraction pattern with this method. EBSD uses low energy electrons, and the diffraction patterns it yields when successful only reflect the orientation at the surface of the sample being studied. If there is any significant damage to the surface of the material, such as a layer of worked material left from the polishing process, EBSD will be ineffective. The difficulty of preparing Aluminum 5052 for examination EBSD

has been documented: to get decent diffraction patterns, one team of researchers needed to combine steps of hand polishing, vibratory polishing and a final chemical etch through trial and error.[1] For this work, attempts at EBSD were abandoned when it was realized that it would be easier to attain the data of interest with X-ray diffraction methods.

2.7 X-ray Diffraction

The specimens in the mounts were examined with X-ray diffraction on a Bruker D8 Discover X-ray diffractometer. Bruker General Area Detector Diffraction Software (GADDS) running on a Microsoft Windows computer workstation was used to analyze the resulting data. The back of each mount was stuck to an aluminum post using double-sided adhesive tape, and the aluminum post was clamped into a fixture on the stage of the D8's goniometer. The D8's goniometer could rotate about three axes: ω, ϕ, and χ. With the general area detector of the D8 centered at 2θ values of 51°, the detector observed arcs of the Debye rings from the {111}, {200}, and {220} planes in the grains of the aluminum metal. The X-ray generator was run at a voltage of 40 kV and a current of 40 mA. Many 'frames' of X-ray data were automatically gathered, according to a scheme, to acquire data to generate pole figures from. A scheme consisted of a series of steps, each step defined in terms of the following parameters: 2θ, ω, ϕ, χ, the axis of rotation, the frame width, the number of frames, and the exposure time of each frame. To execute any given step of the scheme, the goniometer and detector would drive to the given angles, and the goniometer would proceed to rotate about about the specified axis of rotation. The goniometer stage rotated continuously at an angular rate equal to the frame width divided by the exposure time and the X-ray shutter and detector operated in such a way as to capture distinct frames at intervals of the exposure time, until the specified number of frames had been captured. The scheme used in this work is presented in Table 2.7.

After capturing the set of frames specified by the scheme, the GADDS software was used to automatically generate pole figures for the {111}, {200}, and {220} poles.

2θ	ω	ϕ	χ	Axis	Frame width	#Frames	Exposure Time
51	25.5	0	70	ϕ	2.5°	144	5s
51	25.5	0	50	ϕ	2.5°	144	5s
51	25.5	0	90	ω	0.5°	16	5s

Table 2.1: Table of the pole figure data gathering scheme parameters

Chapter 3

Results

3.1 Qualitative Description of Forming Results

The forming process successfully bulged the workpieces. The resulting shapes of the workpieces, however, were unexpected. In workpieces formed prior to this work on the same apparatus, the forming process had resulted in a shape that appeared conical, and radially symmetrical to the eye. The workpieces formed for this work lacked the appearance of radial symmetry after forming, but both did appear to have mirror symmetry along a diagonal of the square sheet of metal. The bulges in the workpieces, though asymmetrical, also had a more domed than conical shape. In both workpieces, sides of the original square, with the apparent mirror plane along the diagonal between them, had been pulled inwards, with crumpling in the middle of those sides. In the annealed workpiece, this only appeared on two of the sides, while the other two sides appeared to have remained mostly straight and un-crumpled. In the unannealed workpiece, all four sides of the workpiece were affected: two adjacent sides were pulled in and crumpled to one degree, and the other two adjacent sides were pulled in and crumpled to a degree that was much less but still easily visible. Based on the appearance of the grids on the workpieces, highest points on the workpieces also seemed to be the most strained areas. Photographs of the formed workpieces are presented in Figure 3-1, though it is difficult to see the extent of the asymmetry in the photographs.

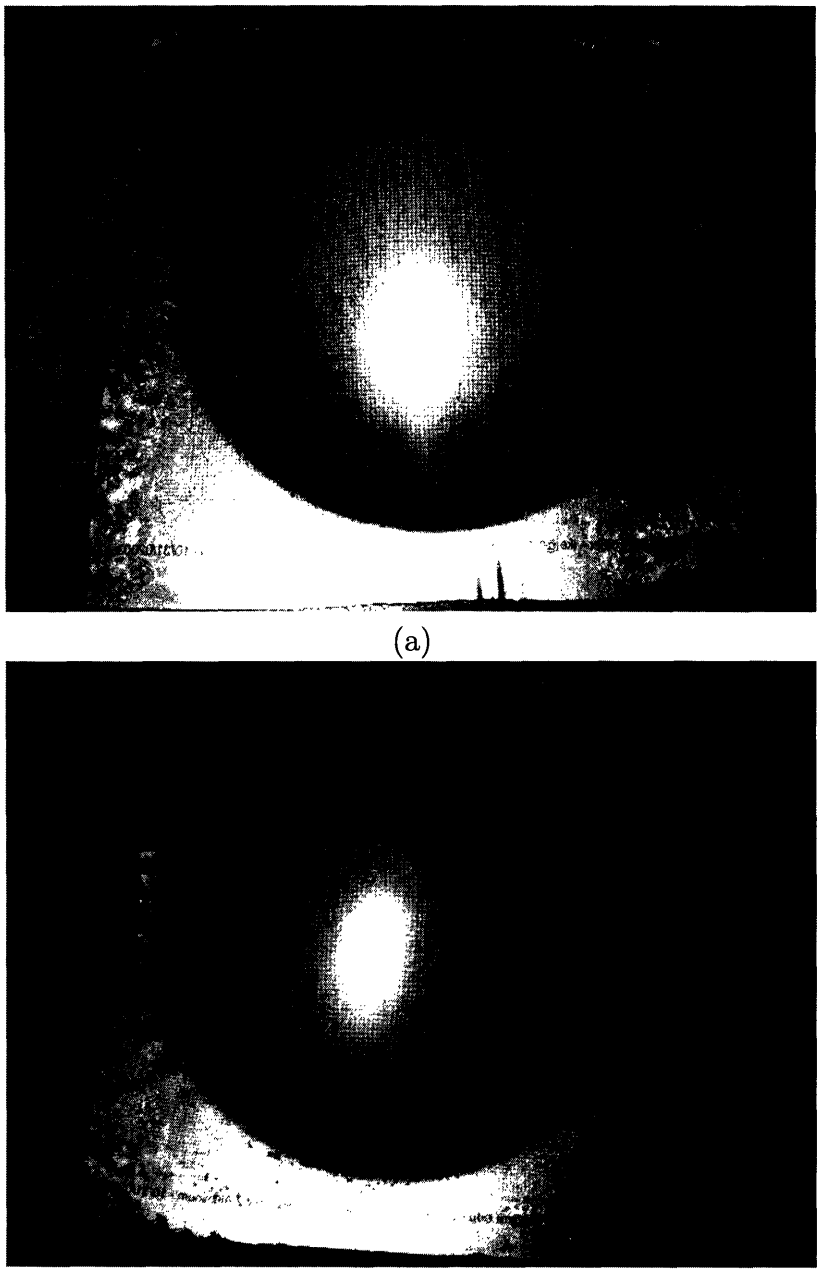

(a)

(b)

Figure 3-1: The formed workpieces: (a) The unannealed workpiece, (b) The annealed workpiece

Workpiece	ϵ_x	ϵ_y	ϵ_z	$\epsilon_{effective}$
Annealed	0.16	0.20	-0.17	0.35
Unannealed	0.12	0.1	-0.08	0.19

Table 3.1: Strain measurements and calculated effective strain

3.2 Electrical Monitoring of Forming Process

By inspection of a graph of the current and voltage of the electrical pulses used to do the forming, the duration of a typical pulse is estimated to have been 500 microseconds.

3.3 Strain Measurements

Measurements were taken at the peaks of the workpieces, which were assumed to be the most strained areas of the workpieces. Distance measurements from the strained areas and from the unstrained grid were used to calculate true strains in the transverse, rolling, and thickness directions: ϵ_x, ϵ_y, and ϵ_z respectively. Strain measurements and the calculated effective strain for each workpiece are presented in Table 3.1; the following formula was used to estimate von Mises effective strains based on those measurements:

$$\epsilon_{effective} = \frac{1}{\sqrt{2}}\sqrt{(\epsilon_x - \epsilon_y)^2 + (\epsilon_x - \epsilon_z)^2 + (\epsilon_y - \epsilon_z)^2}$$

3.3.1 Strain Rate Estimate

The time scale of the forming event is guessed to be very close to the duration of a typical electrical pulse used in forming. Using the estimates of effective strain, the strain rate for the peak of the annealed workpiece is estimated to have been on the order of 700/s and the strain rate for the peak of the unannealed workpiece is estimated to have been on the order of 380/s.

3.4 Optical Microscopy

3.4.1 Pre-etch micrographs

After polishing, scratches and other features were visible under the microscope, especially at high magnification. See Figure 3-2. The most noticeable features were darker gray shapes, elongated and rectangular in the unannealed specimens (Figure 3-2(a),(c)). The gray shapes were aligned parallel to the rolling direction of the metal. In the annealed, unformed specimen (Figure 3-2(b)), the gray shapes are rounded and appear unaligned with any direction or with each other. The annealed, formed specimen (Figure 3-2(d)) showed elongated gray shapes aligned with the rolling direction like both of the unannealed specimens. On all the specimens, small dark dots were visible, but in much greater numbers on the formed specimens than on the unformed specimens.

3.4.2 Post-etch micrographs

Etching successfully made the grain structure of the metal visible under crossed polarizers on an optical microscope. See Figure 3-3. The levels of contrast appear different between the micrographs of the unformed and formed specimens because different polarizing filters were used. On all specimens, a lot of pitting was apparent. At high magnifications, it was evident that many of the pits had shapes similar to the dark gray shapes that were visible on the specimens before etching. The annealed unformed specimen (Figure 3-3(b)) showed quite a lot of pits aligned in some direction, but this direction was not the rolling direction. No immediate correlation between grain shape and whether the specimen was formed or not was apparent in the micrographs. In the unformed specimens, the grain size appeared much greater in the annealed specimen than in the unannealed specimen. In the formed specimens, the grain size appeared only a little bit larger in the the annealed specimen than in the unannealed specimen.

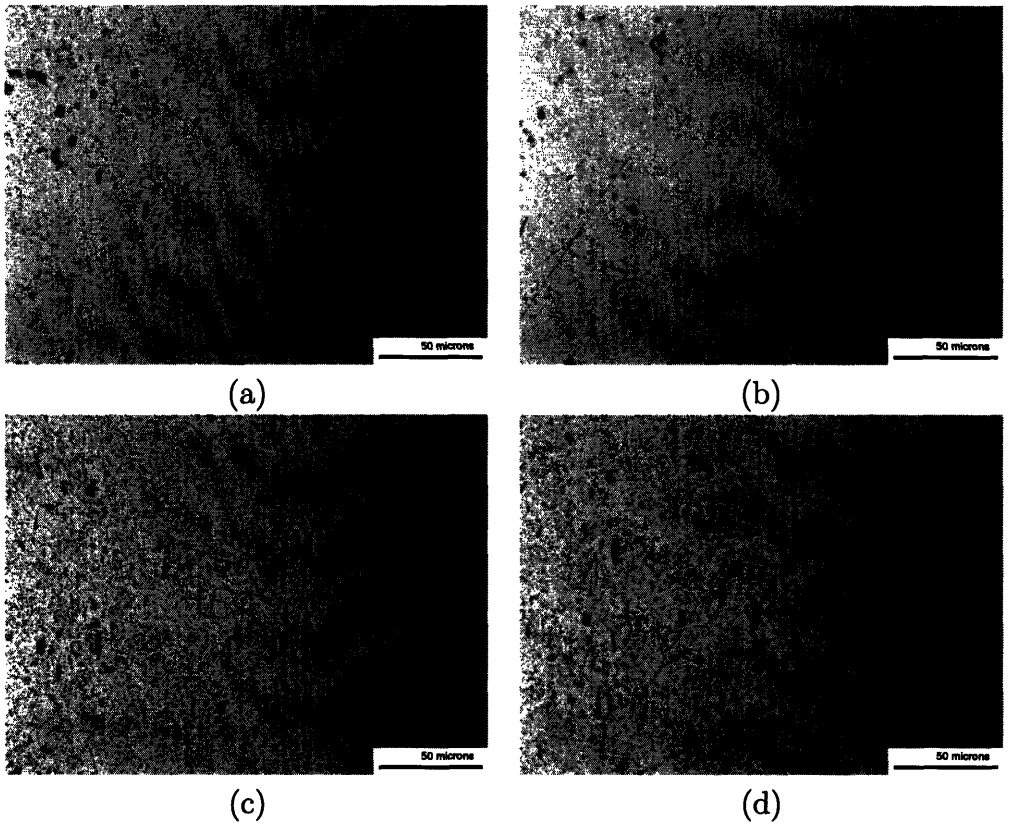

Figure 3-2: Micrographs of the polished, unetched surfaces of four specimens: (a) The unannealed, unformed Aluminum 5052, (b) The annealed, unformed Aluminum 5052, (c) The unannealed formed specimen, (d) The annealed formed specimen.

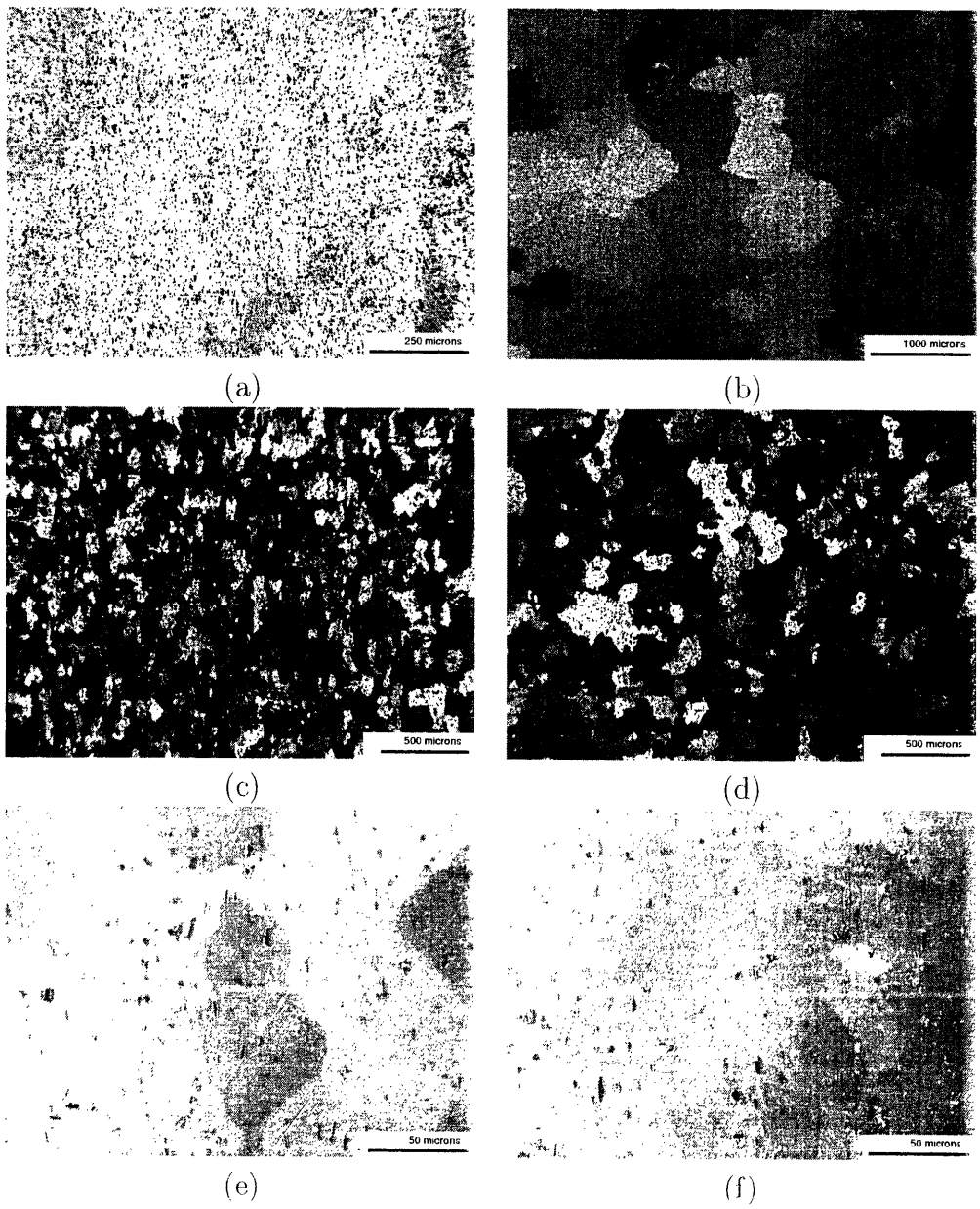

Figure 3-3: Micrographs of the etched surfaces of the four specimens, taken with crossed polarizers. (a) The unannealed, unformed Aluminum 5052, (b) The annealed, unformed Aluminum 5052, (c) The unannealed formed specimen, (d) The annealed formed specimen, (e) A higher magnification view of the unannealed formed specimen, (f) A higher magnification view of the annealed formed specimen.

Specimen	Grain size (μm)
Unannealed Unformed	34
Annealed Unformed	470
Unannealed Formed	41
Annealed Formed	97

Table 3.2: Measured average grain sizes of the specimens.

3.4.3 Calculation of average grain size

The linear intercept method was used to calculate the average grain size of the specimens from micrographs taken of them. In the linear intercept method, a line of known length is drawn across the micrograph, and the number of grain boundaries it crosses is counted. The length of the line is divided by the number of grain boundaries crossed to produce an estimate of the average grain size. Multiple lines can be drawn across the image to attempt a more accurate measure. The lines for measuring the average grain sizes for these specimens were drawn horizontally across the micrographs, perpendicular to the rolling direction. The measured grain sizes for these specimens are presented in Table 3.2.

3.5 X-ray diffraction

3.5.1 General Observations

In the process of gathering X-ray diffraction data to generate pole figures for the specimens, the annealing state of the specimens had a distinct and very noticeable effect on the X-ray diffraction patterns. Unannealed specimens showed distinct arcs of Debye rings on the detector of the diffractometer, with smoothly varying intensity along the length of the arcs. Annealed specimens, on the other hand, only showed discrete points of intensity at various spots on the detector. These points of intensity fell on the Debye rings for the material, but were separated by large regions of only background-level X-ray counts.

3.5.2 Texture Analysis

The scheme for gathering pole figure data did not collect complete pole figures due to geometric constraints. Capturing the data to complete the outer regions of the pole figures would have required tilting the specimen at high angles to the X-ray beam. The beam would have spread off the specimen being examined and diffracted off the copper in the mount, and at some angles, the detector itself would be partially in the shadow of the X-ray beam cast by the mount.

The X-ray data from the unannealed specimens yielded pole figures showing distinct preferred orientations in the {111}, {200}, and {220} poles. See Figure 3-4. The pole figures for the formed unannealed specimen were less intense than for the unformed unannealed specimen, but other than that, there was not much difference between them.

The X-ray data from the annealed specimens were also processed into pole figures, but the pole figures generated do not show any preferred orientation. See Figure 3-5. Both sets of pole figures appeared to show a random distribution of orientation. The pole figures for the formed annealed specimen were more blurry than for the unformed specimen.

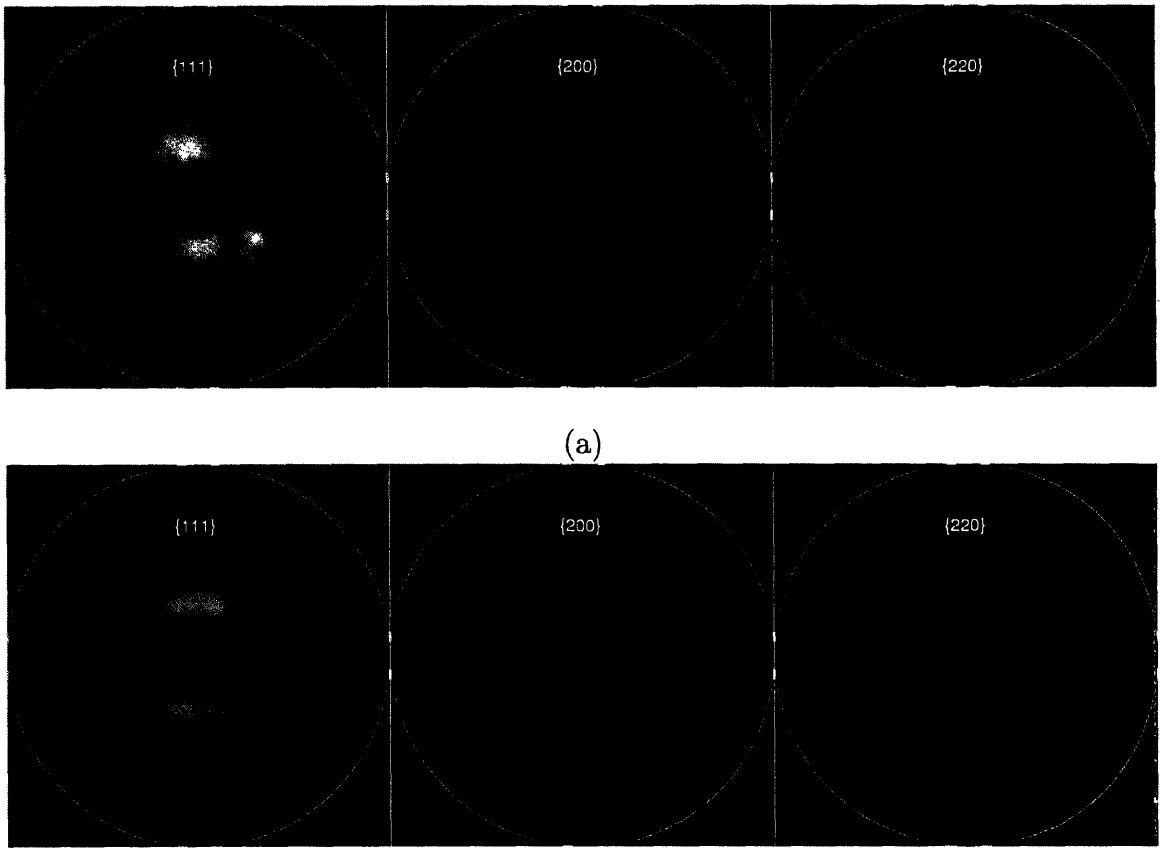

Figure 3-4: X-ray diffraction pole plots of the {111},{200}, and {220} poles for (a) a specimen of unannealed, unformed Al 5052 metal, and (b) a specimen taken from the unannealed, formed workpiece.

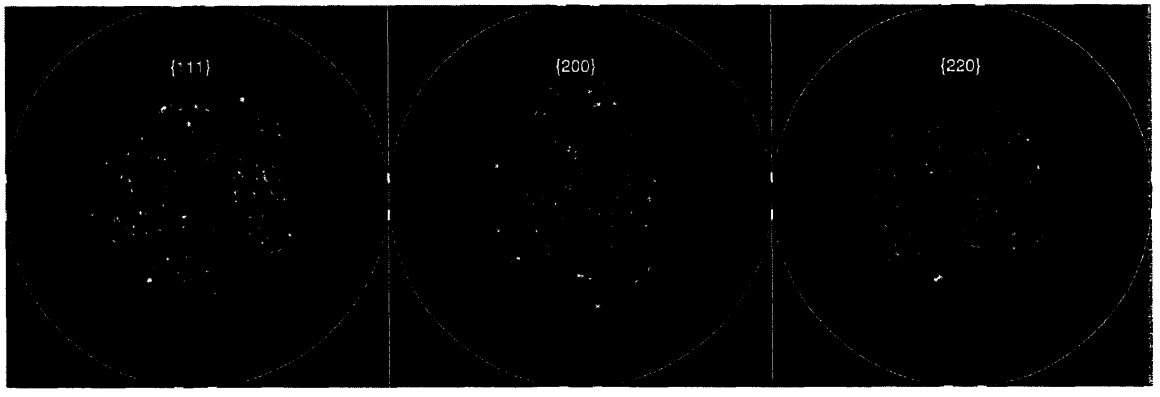

(a)

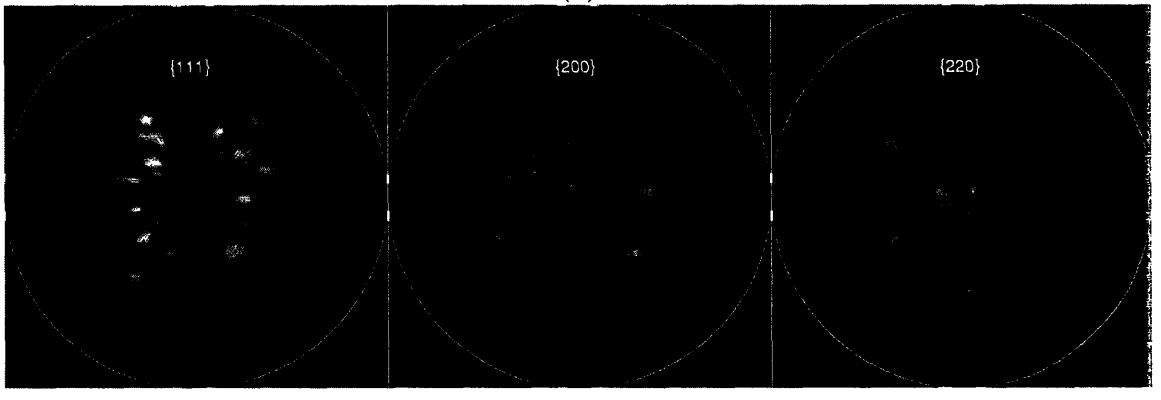

(b)

Figure 3-5: X-ray diffraction pole plots of the {111},{200}, and {220} poles for (a) a specimen of annealed, unformed Al 5052 metal, and (b) a specimen taken from the annealed, formed workpiece.

Chapter 4

Discussion

4.1 Unexpected Forming Results

The lopsided shapes of the formed workpieces were unexpected, but there are a few factors that could have been responsible for those results. The uneven domed shapes of these formed workpieces, as opposed to the conical and symmetrical shapes of workpieces formed previously on the same apparatus, imply that one or several conditions were different when forming these workpieces. The differences might have been in the distribution of clamping forces of the laboratory press holding the forming apparatus together, the bulk properties of the workpiece material, or the surface conditions of the workpiece material.

If the upper and lower platens of the laboratory press were not adequately aligned or the pressure vessel, workpiece, and expansion tube were not well centered within the laboratory press, the clamping force exerted by the press might have been unevenly distributed across the workpiece, allowing some sides to slip and be pulled in during forming. Care was taken to align all of the parts of the system properly before forming, but misalignment cannot be ruled out as a cause of the unexpected forming results.

The workpiece material for this project was 0.040 inch thick mirror finish Aluminum 5052 sheet metal from McMaster-Carr industrial supply. The workpiece material for the previous project was also 0.040 inch thick Aluminum 5052 sheet metal,

but with a satin finish. It is conceivable that the surface finish, or the processing used to apply that finish to the workpiece, may have an affect on the bulk mechanical properties of the sheet metal. Annealing the workpieces for this project also suggested some difference between them and the workpieces used in the previous project, as described in the Materials section of the Experimental Methods chapter.

Besides the differences between the mirror finish of the workpieces for this work and the satin finish of the workpieces for the previous project, the surfaces were also treated differently prior to forming. For this project, as described in the experimental section, the workpieces were covered with a film to make a grid of points for mapping the strain imparted by the forming. This film of plastic was thin with respect to the thickness of the metal workpieces, and had much much lower tensile strength, so it is unlikely that it played much of a role in the unexpected shapes of the formed workpieces in this project, but it is still possible.

4.2 Strain Measurement

The grids applied to the formed workpieces in this work were useful enough for rough measures of strain, but left a lot to be desired due to the imperfect nature of the transfer, and the difficulty of making precise and accurate measurements. Because of the curvature of the workpieces, and because the amount of strain varied continuously from the center to the edge of the workpieces, increasing the distances between grid points would rapidly reduce the accuracy of the strain measurement, even though it would also reduce the percent error. The most accurate strain measurements would be the ones conducted over the smallest feasible distances.

One of the original aims of this work had been to produce two-dimensional maps of the strain across the surfaces of the workpieces, to see if visualizing the strain levels across the workpieces might lead to some insight. Because of the problems with the grids and the difficult nature of measuring strains from the workpieces, this was impractical.

In future work of this nature, it would be useful to consider other methods for

attaining precise grids on the workpieces, as well as other methods for measuring those grids. A pen plotter might be used to draw a grid with permanent markers, or a laser might be used to ablate a grid pattern out of a thin coating on the workpiece without damaging the workpiece. Photography or laser scanning and computer processing could conceivably automate the process of mapping the strain across a workpiece, but such methods would not be trivial to develop.

4.3 Interpretation of Micrographs

The gray shapes visible in the micrographs of the unetched specimens are assumed to be second-phase constituents (precipitates) because of their ubiquity and their alignment with the rolling direction of the metal in the uannealed specimens. That these second-phase constituent particles are rounded and unaligned with the rolling direction in the annealed, unformed specimen (Figure 3-2(b)), while they are still elongated and aligned with the rolling direction in the annealed, formed specimen (Figure 3-2(d)) suggests that the metal of the annealed workpiece that was formed did not anneal to the same extent that the metal of the unformed specimen did. This is very unusual, because all the annealed metal used in this work was annealed simultaneously, and for long enough to assure even and thorough heating of the metal. The presence of more small dark dots on the formed specimens than the unformed specimens does not immediately suggest an explanation, except that something about the strained condition of the metal of the specimens from the formed workpieces makes that metal more susceptible to mechanical pitting during polishing.

Using the Barker's Etch on the samples to reveal the grain structure was successful, but always left the sample covered with small pits. These pits appeared to have approximately the same size, shape, and quantity per area as the gray shapes visible in the micrographs of the specimens taken prior to etching, so it seems that the etch preferentially attacked the material of these gray shapes. This supports the hypothesis that the gray shapes were constituents of a second phase in the metal.

The grains in the unannealed specimens are elongated in the rolling direction like

the gray shapes. In the annealed, unformed specimen, the grains have grown quite substantially, and are no longer aligned with the rolling direction. The annealed, formed specimen has larger, less elongated grains than either of the unannealed specimens, but the difference is not very substantial; this also supports the hypothesis that the metal in the annealed, formed specimen did not anneal as much in the annealed, unformed specimen. The biaxial stretching from the electrohydraulic forming process does not appear to have changed the grain shape in any easily identifiable way.

4.4 Pole Figures

Although the micrographs suggest that the annealed, formed specimen might be more like the unannealed specimens than the annealed, unformed specimen, the results of the X-ray diffraction indicate otherwise: the pole figures from the annealed, formed specimen bear no resemblance to the pole figures from the unannealed specimens. None of the pole figures from the annealed specimens show any preferred orientation. The difference in the extent of annealing, however, is also apparent in the pole figures. The annealed, unformed sample yielded pole figures with very small points of intensity, which indicate that the X-ray beam in the diffractometer was only hitting a few single-crystal grains in the specimen. This fits with the large grain size found in the annealed, unformed specimen. The broader, more blurry points of intensity in the pole figures from the annealed, formed specimen are consistent with a smaller grain size, such that the X-ray beam was diffracted off more of them.

As mentioned before in the Results chapter, there seems to be little difference between the pole figures from the formed and unformed unannealed specimens, other than the overall intensity. This suggests that the high strain rate biaxial deformation did little to change the texture of the metal. These results could be compared with results obtained by Banovic and Foecke, who reported pole figures from as-recieved (uannealed and unformed) Aluminum 5052 and from unannealed Aluminum 5052 strained to levels of 0.104 and 0.198 by equibiaxial stretching at a slow strain rate. [8]

Banovic and Foecke obtained pole figures by neutron diffraction, which exposes the entire volume of a specimen to a neutron beam, and allows entire pole figures to be determined. The texture throughout the specimen must be homogenous, however, and the volume of the specimen must be at least 8 mm^3. To use the neutron diffraction technique with sheets of metal thinner than 2 mm, then, a stack of flat pieces of the metal is made to make up a uniform volume.[1] Because the electrohydraulic forming process necessarily imparts non-negligible curvature to entire biaxially stretched area of the workpiece, and because the strain varies continuously over that area as well, stacking specimens from elctrohydraulically formed workpieces would not be suitable for analysis with neutron diffraction. Banovic and Foecke's pole figures all appear generally similar to the pole figures reported here, but there are more easily discernible differences between their pole figures from different strain levels.

Chapter 5

Conclusions

Aluminum workpieces were successfully stretched biaxially at high strain rates, but analyzing specimens did not show a noticeable correlation between the forming process and the microstructure or the crystalline texture. Because the crystalline texture of the unannealed metal appeared unchanged by the forming process, it might be hypothesized that at high strain rates, the inertial effects thought to be responsible for delaying failure might also inhibit grain reorientation. Repeating the experiment and attempting to acquire more complete and more detailed pole figures could help support or disprove this hypothesis. Investing the time to develop polishing techniques and skills good enough to use EBSD on the specimens might also lead to more interesting results.

The experimental results were also very illustrative of the effects of annealing on these parameters: the unformed annealed specimen became morphologically isotropic and lost any preferred crystallographic orientation, and the formed annealed specimen, which for some reason seemed less annealed than the unformed specimen, lost any preferred crystallographic orientation but retained it's morphological anisotropy.

Appendix A

Concerning the Electrohydraulic Forming Apparatus

A.1 Overview

The electrohydraulic forming apparatus used for this work was previously used for a group project in the class 3.082: Materials Processing Laboratory at the Massachusetts Institute of Technology in the spring of 2003. The apparatus consisted of a custom designed and fabricated pressure vessel and electrode assembly, a Carver® bench-top laboratory press, and an old Magneform electromagnetic forming machine as the source of the power current pulse necessary to produce an electrohydraulic explosion.

A.2 The Pressure Vessel

The pressure vessel was a hemispherical cavity 6 inches in diameter, bored out of a 8" diameter, 5" tall cylinder of AISI 1045 medium carbon steel. This was modeled as a thick-walled pressure vessel with an inner radius of 3" and an outer radius of 4". With the tensile yield strength of AISI 1045 steel given on a data sheet as 55,000 psi, this shape is calculated to yield at a pressure of a little more than 34,000 psi. The vessel was pierced by two holes on opposite sides of the vessel, which copper

electrodes surrounded by a thick layer of Teflon® passed through.

A.3 The Electrodes

The electrodes consisted of 3/16" copper rods pushed through holes drilled through 1/2" Teflon® rods. The Teflon® was used to insulate the copper electrically from the walls of the pressure vessel. The copper rods were prevented from sliding out of the vessel under pressure by a steel pin through each rod, against a washer, against the Teflon® insulation. 5/16" diameter holes for the Teflon®/copper assembly were drilled through solid stainless steel pipe plugs which screwed into the holes for the electrodes on the outside of the pressure vessel. The Teflon® on part of each electrode was turned down to be a tight fit in the pipe plugs. This design was adopted to prevent the electrodes from being ejected from the pressure vessel during an explosive firing.

A.4 The Magneform

The machine supplying the current pulse for the electrohydraulic forming was a Magnform Mark I, manufactured by the General Atomic division of General Dynamics sometime before 1966. The Magneform was essentially a large capacitor bank designed to enable electromagnetic forming by dumping up to 6 kilojoules of energy through one of many interchangeable forming coils. To harness the energy output of the Magneform for electrohydraulic forming, the electrodes in the pressure vessel were connected to the Magneform in parallel with one of the Magneform's largest work coils by means of leads connected to copper plates inserted into the Magneform's terminal. A grounding lead was also attached from the case of the Magneform to a wing nut on the body of the lab press. Each lead was a thick black neoprene-jacketed cable containing 5 separate 10-gauge stranded copper wires. At the ends of each lead, the copper wires were stripped about 3/4" and gathered together, and clamped in a lug fastener. The forming coil was left in parallel with the pressure vessel to avoid damage to the Magneform in case the energy of the Magneform failed to be

discharged through the pressure vessel. This meant that some portion, possibly a large portion of the energy released by the Magneform was dissipated by the forming coil instead of contributing to the electrohydraulic explosion in the pressure vessel, but the electrohydraulic explosions produced by this method were quite sufficiently large as they were. Voltage and current measurements taken during firing suggested that about 1 kilojoule of energy was being dissipated through the pressure vessel.

A.5 Forming Methods

For most firings of the Magneform, the pressure vessel assembly in the laboratory press consisted of the vessel, neoprene gaskets, the workpiece, and a 6" I.D., 8" O.D., 5" tall Aluminum 6061 tube with a 1" hole in it's side for the workpiece to expand into. A silicon bronze die was also prepared in the course of the class project, and forming was conducted with the die in the system as well. When forming with the die, the die went on top of the workpiece, and the aluminum expansion tube went on top of the die. A vacuum line was connected to the die through the hole in the aluminum tube, and a rough mechanical vacuum was pulled on the system during firing.

To fire the system, a thin brass bridging wire was placed between the electrodes inside the pressure vessel. The pressure vessel was then filled with water. A gasket made of neoprene rubber sheet was laid down on top of the pressure vessel, and then the workpiece was placed on top of that, with care taken to center the workpiece on the vessel. A second neoprene gasket was placed on top of the workpiece, and then the die or expansion tube was placed on top of the gasket. A clamping force of 12,500 pounds was applied to the system with the laboratory press. The electrical monitoring system was then cued, and the Magneform machine was powered on and fired. After firing, the Magneform was turned off, the clamping force was released on the lab press, and the pressure vessel assembly was taken apart to access the formed workpiece.

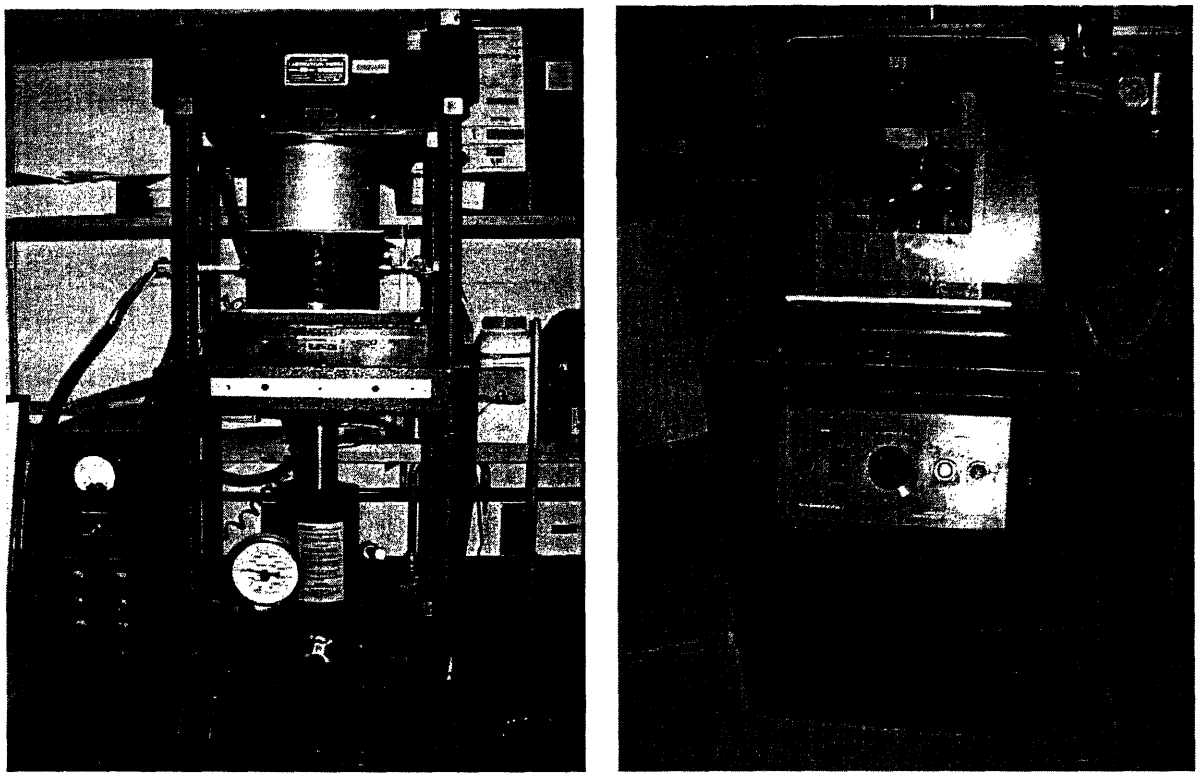

(a) (b)

Figure A-1: (a) The pressure vessel assembly clamped up in the lab press. Visible are the pressure vessel, the ends of the electrodes, the workpiece, the gasketing, the expansion tube, and the leads to the Magneform. (b) The Magneform Mark I, with leads to the pressure vessel and the electrical monitoring system in place.

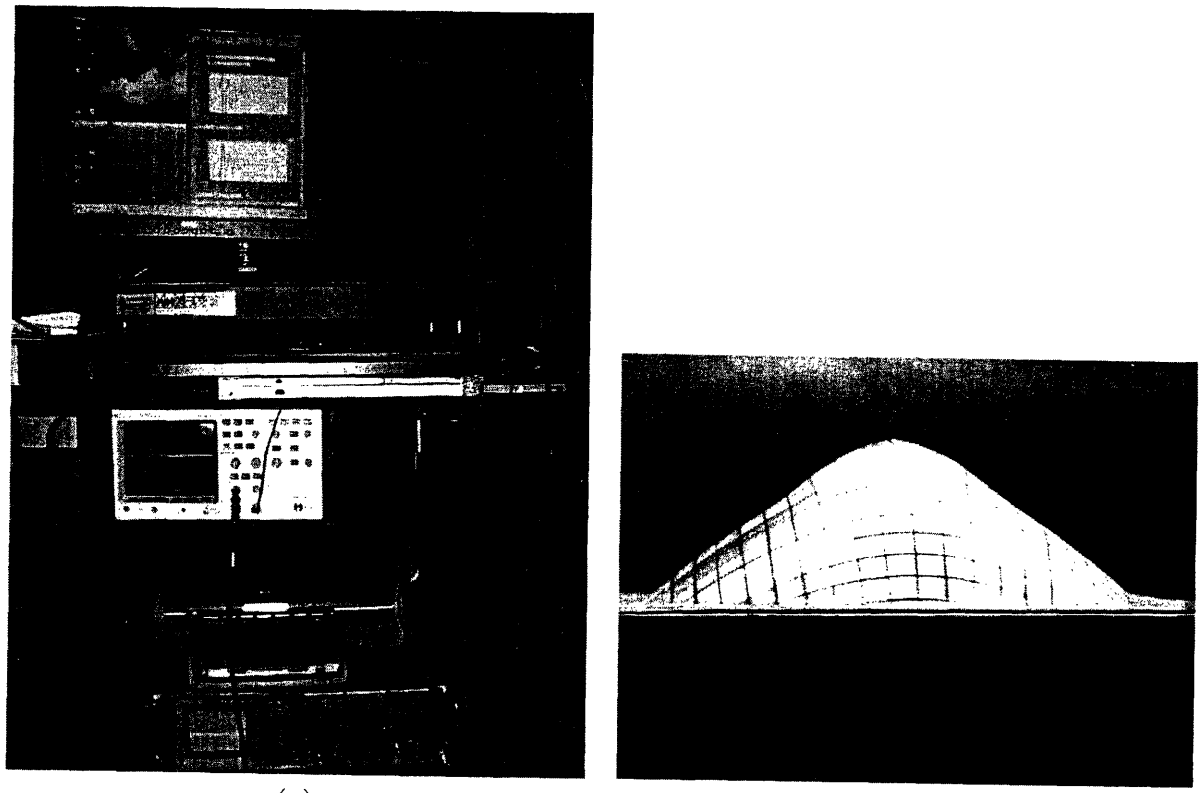

(a) (b)

Figure A-2: (a) The system of oscilloscopes and a computer used to capture electrical data about the firing of the magneform. (b) An annealed workpiece that was formed with the expansion tube.

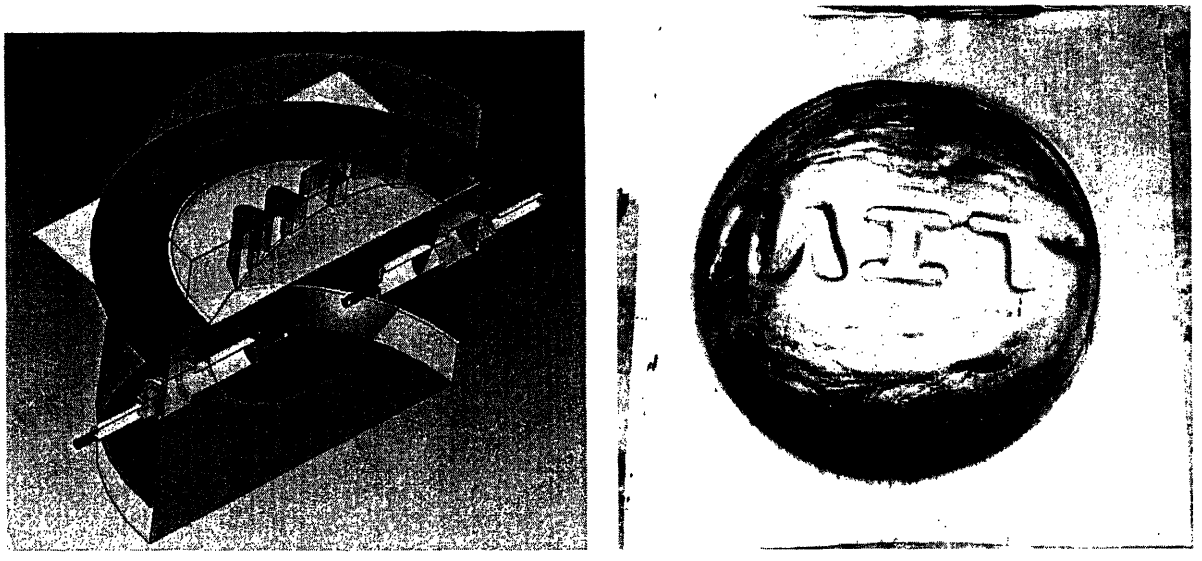

(a) (b)

Figure A-3: (a) A cross-sectional rendering of the pressure vessel assembly, with the die in place. Also represented are the gaskets and the electrode assemblies. Image by Hao Hu. (b) A workpiece after being electrohyrdraulically formed into the die.

Bibliography

[1] S.W. Banovic, M.D. Vaudin, T.H. Gaeupel-Herold, D.M. Saylor, and K.P. Rodbell. Studies of deformation-induced texture development in sheet materials using diffraction techniques. *Materials Science and Engineering A*, 380:155–170, August 2004.

[2] Jong-Jin Park. Predictions of texture and plastic anisotropy developed by mechanical deformation in aluminum sheet. *Journal of Materials Processing Technology*, 87:146–153, 1999.

[3] P.J. Maudlin and S.K. Schiferl. Computational anisotropic plasticity for high-rate forming applications. *Computer Methods in Applied Mechanics and Engineering*, 131:1–30, 1996.

[4] J.R. Bowen, Prangnell P.B., and F.J. Humphreys. Microstructural evolution of the deformed state during severe deformation of an ecae processed al-0.13 *Materials Science Forum*, 331-337:545–550, 2000.

[5] R. Davies and E. R. Austin. *Developments in High Speed Metal Forming*, chapter 3.2 Electrohydraulic Forming, pages 225–252. Industrial Press Inc., New York, NY, 1970.

[6] *Properties of Wrought Aluminum and Aluminum Alloys*, volume 2, Properties and Selection: Nonferrous Alloys and Special-Purpose Materials of *ASM Handbook*, chapter 5052 (2.5Mg-0.25Cr). ASM International, ASM Handbooks Online, http://www.asmmaterials.info, 2002.

[7] Richard H. Stevens. *Aluminum Alloys: Metallographic Techniques and Microstructures*, chapter Microexamination. ASM Handbook. ASM International, ASM Handbooks Online, http://www.asmmaterials.info, second edition, 2004.

[8] S.W. Banovic and T. Foecke. Evolution of strain-induced microstructure and texture in commercial aluminum sheet under balanced biaxial stretching. *Metallurgical and Materials Transactions A*, 34A:657–671, March 2003.

[9] Toshimi Tobe, Masana Kato, and Haruki Obara. Dynamic plastic deformation of circular metal sheets subjected to impulsive pressure by underwater wire explosions. *Institute of Physics Conference Series*, 47:383–393, 1979.